National Energy Technology Laboratory
NETL Journal of Energy and Environmental Research
Vol. 1, No. 1 (2001), 91-103

Non-Isothermal Simulation of Gas Flows In the Hot-Gas Filter At Wilsonville

Isaac K. Gamwo,[1] Goodarz Ahmadi[2], John S. Halow, [3] and Edward J. Boyle[3]
[1] U.S. Department of Energy
National Energy Technology Laboratory
P.O. Box 10940, Pittsburgh, PA 15236-0940
gamwo@netl.doe.gov, Tel. (412) 386-6537; Fax: (412) 386-5936

[2] Department of Mechanical and Aeronautical Engineering
Clarkson University, Postdam, NY 13699

[3] U.S. Department of Energy
National Energy Technology Laboratory
P.O. Box 880, , Morgantown, WV 26507-0880.

Abstract

A numerical simulation of non-isothermal gas flows in the hot-gas filter vessel at the Power Systems Development Facility in Wilsonville, Alabama is presented. The gas velocity and thermal simulations are based on the Reynolds Stress Transport Turbulence Model of the FLUENT™ code. While most earlier modeling studies were limited to isothermal conditions, in this study, the energy transport equation was solved in addition to the mass and momentum equations. The gas flow and temperature field inside the filter vessel was also studied. Results reveal that the gas flow shows strong rotating flow regions outside the shroud and in the upper and lower parts of the body of the vessel. It is also shown that the temperature distribution is non-uniform with somewhat higher temperatures in the upper part of the filter. The simulation results are compared with the experimental field observations of the filter vessel.

Nomenclature

k turbulence kinetic energy
p gas pressure
P fluctuating kinetic energy production
R Reynolds stress tensor
t time
T gas temperature

u gas velocity vector
u' gas fluctuating velocity vector
x axial coordinate

Greek Letters
α thermal conductivity
δ unit tensor
ε rate of dissipation of kinetic energy of turbulence
ϑ kinematic viscosity
ν viscosity
ρ mass density
σ turbulent Prandtl number

Subscripts
i,j,k coordinate directions
t turbulent (prefix)

Superscripts
k for turbulence kinetic energy
T for temperature
ε for rate of dissipation of kinetic energy of turbulence
- mean

1. Introduction:

The use of ceramic candle filters for hot-gas filtration has attracted considerable attention. Candle filters have a diameter of about 6 cm and a length of 1 to 1.5 m, and with the wall thickness of about 1 cm. An industrial unit normally contains a large number of candle filters. During the operation of the filter vessel, the hot gases pass through the walls of the cylindrical filters, and the filtered particles form a cake on the outside of each filter. Groups of candle filters are periodically cleaned by a rapid (reverse-flow) pulseback procedure to remove the transient cake that builds up on filter surfaces. A number of hot-gas filtration systems were developed and tested in the past.

Under ideal conditions, when hot-gas filtration systems operate as intended, they produce stable, minimal pressure drops across the filtration system; effectively remove fine particles and deliver essentially particulate-free hot gases that meet turbine engineering requirements and regulatory standards for power-plant emissions (Lippert et al., (1995), Radian (1994)). Each cleaning pulse removes the transient cake from each filter leaving only a residual cake, and the problems of ash bridging and/or incomplete removal of filter cakes do not occur. On occasions, however, the pressure drop across the tube sheet may not reach a small, steady state value, but increases continuously. When particle-deposits build up in a filter vessel, the routine logging pressure drops across the tubesheet usually provides an indication of an operating problem.

Monotonically increasing pressure drops imply that particulate cakes are building up on and/or around the filters. "Filter bridging" occurs when all of the space between adjacent filter surfaces has been filled by particles. Smith and Ahmadi (1998) suggested, among other hypotheses, that "filter bridging" is caused by particle depositing on solid surfaces (tubesheets and central post) that have no cleaning mechanisms. In addition, the incomplete filter cleaning, in which within each cycle the amount of cake removed is slightly less than the amount of new cake formed was suggested as another potential mechanism. In this case the average filter-cake radius slowly expands until cakes on adjacent filters meet.

Development of experimentally verifiable computer models to simulate the gas flow and particles deposits in the filter vessel will provide an important tool for design of future industrial scale filtration systems (Ahmadi and Smith (1998), Ahmadi and Zhang (2000), Zhang and Ahmadi (2001)). For subsequent experimental, theoretical, engineering, and modeling efforts, it is important to know the mechanisms by which ash deposition occurs as well as the major locations of particle deposition. When filter cakes are the only important deposits, the model of Smith et al. (1998), when combined with data such as obtained by Dahlin et al. (1998) and Kono et al. (1998), gives quantitative answers for the time dependence of the filter cake thickness. When combined with laboratory (Kono et al. (1998), Smith et al. (1997a)) and operating data (Smith et al. (1997b)), the model of Ferer and Smith (1998) eventually may be of direct engineering use for solving the problem by improving filter cleaning.

To design effective and reliable hot-gas cleaning filtration systems, a fundamental understanding of the particle transport and deposition processes in filter vessels is also needed. Currently, modeling of gas flow and particle transport and deposition is one important technique available for advancing our knowledge on the mechanism by which particle deposits begin and grow.

Computer simulations of the hot gas filtration process were performed by Ahmadi and Smith (1998a). PARTICLE code of Ahmadi and coworkers (Li et al. (1994), He and Ahmadi (1999)) was then used to predict particle deposition patterns. Ahmadi and Smith (1998b) also described a computer simulation study of gas flow and particle deposition in the hot-gas filter vessel at Tidd 70 MWE PFBC Demonstration Power Plant. More recently Ahmadi and Zhang (2000) and Zhang and Ahmadi (2001) reported a detailed computer simulation of the hot-gas filter vessel at the Power Systems Development Facility (PSDF) in Wilsonville, AL, under isothermal conditions.

Temperature variations, however, have been reported in the hot-gas filter vessel at Wilsonville (Guan (2000)) with higher temperatures at the upper portion of the vessel and cooler near the cone. These experimental findings have motivated the present study to include the heat transfer analysis and to improve the previous model of Zhang and Ahmadi (2001). In this study, FLUENT^{TM} computational fluid dynamics software was used to model the non-isothermal gas

flows in the filter vessel. The simulation results for gas flow and temperature distribution are presented and discussed. The results for the gas stream pattern show strong rotating flows between the shroud and the refractory liner and in the body of the vessel. The computed temperature distribution in the vessel shows trends that are qualitatively in agreement with the experimental observation at the Power Systems Development Facility (PSDF).

2. Power Systems Development Facility:

Figure 1 shows the schematics of two advanced coal-fired electricity generating systems, known as Integrated Gasification Combined Cycle (Figure 1, upper part) and Advanced Pressurized Fluidized Bed Combustors (Figure 1, lower part), that are being tested at the pilot-scale Power Systems Development Facility (PSDF) in Wilsonville, Alabama.

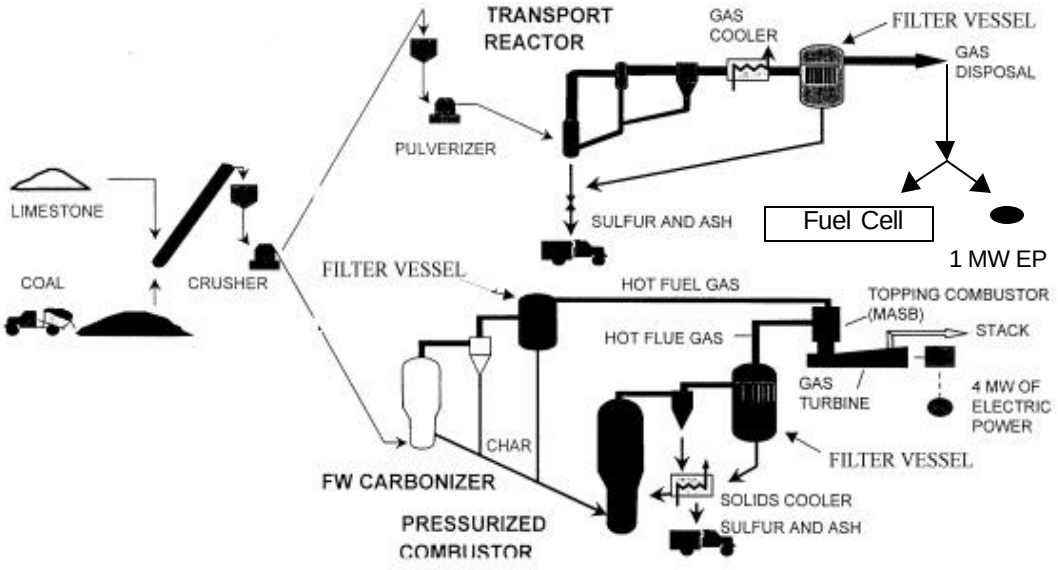

Figure 1. Schematic of the Integrated Gasification Combined Cycle (IGCC) and Advanced Pressurized Fluidized Bed Combustor (APFBC) System at the Power Systems Development Facility in Wilsonville, Alabama.

In the Integrated Gasification Combined Cycle (IGCC) system (Figure 1, upper part) based on the transport reactor, ground coal and limestone are injected into a circulating-transport gasifier/combustor where combustion occurs. The hot gases and entrained fine particles of ash and sulfur pass through a cyclone, which removes large particles. The finer particles that remain then are removed in the filter vessel, so that the cleaning gas be sent through a fuel cell.

In the Advanced Pressurized Fluidized Bed Combustor (APFBC) system (Figure 1, lower part), coal is introduced into a carbonizer, which converts the coal into char and hot combustible gases.

As in the second-generation PFBC, fine particles are removed from the hot gases by a cyclone and filtration unit, the char then is fed into a pressurized combustor, and particles are removed from the hot combustor gases by a second cyclone and a filter vessel. The clean gas exiting from the filter vessels is sent through a hot-gas turbine.

As illustrated in Figure 1, three filter vessels are present at a single site. Here, filtration is performed by cylindrical candle filters, suspended from two plenums inside a pressurized vessel into which the hot gases and suspended particles enter.

3. Wilsonville Hot-Gas Filter Vessel:

A schematic diagram of the Wilsonville filter vessel studied in this paper is shown in Figure 2. Only primary features are illustrated here as the filter has been described in details by Zhang and Ahmadi (2001).

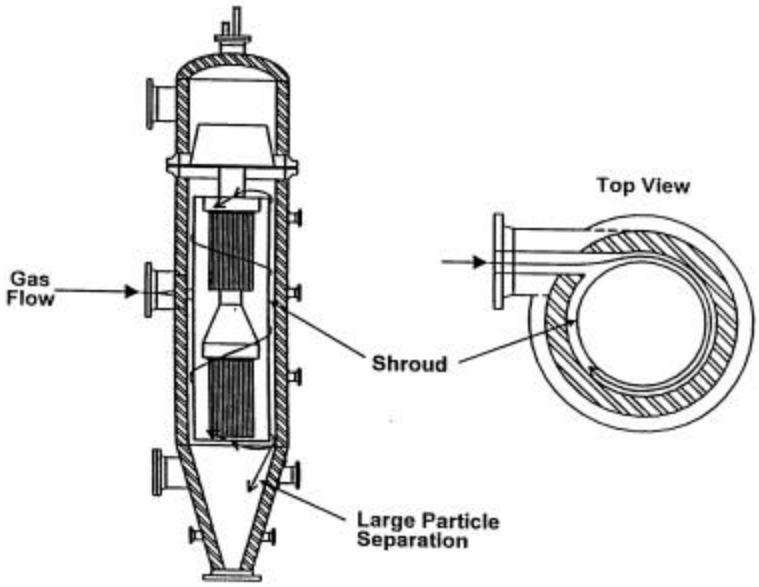

Figure 2. Schematic of the Wilsonville Filter Vessel

The vessel accommodates 91 candle filters arranged in two plenums as shown. The upper plenum has 36 and the lower has 55 candle filters. The ceramic candle filters are about 6 cm (2.36 in.) outer diameter and 1.5 m (4.92 ft) long. The gas enters the vessel tangentially into the shroud. Dust particles are collected on the external surface of the filter, and the dust layer is removed by on-line pulsejet cleaning of compressed air from inside the filter.

4. Simulation Conditions:

The simulated geometry of the filter vessel showing the outlet and conical region is depicted in Figure 3.

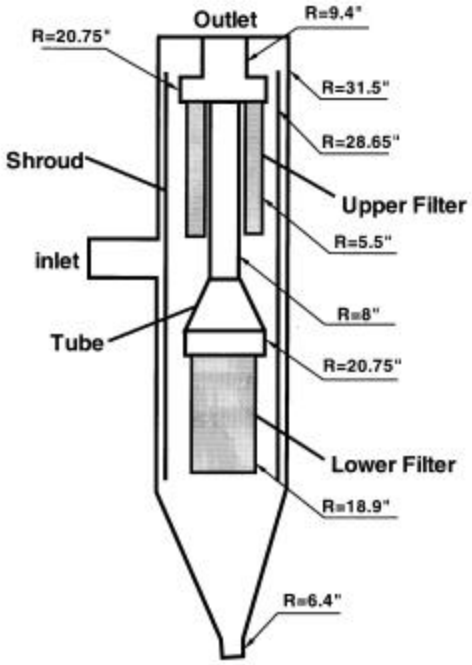

Figure 3. The model of the Hot-Gas Filter Vessel: the dimension of the geometry

Six effective cylindrical filters model the group of filters in the upper tier and the lower cluster of filters is replaced by one effective large cylindrical filter. Each one of the effective filters in the upper tier has outer diameter of 27.94 cm (11 in.) and inner diameter of 23.88 cm (9.4 in.), while the outer diameter of the lower filter is 96.01 cm (37.8 in.) and its inner diameter is 40.64 cm (16 in.). The permeabilities for the upper and lower equivalent filters are respectively $9x10^{-13}$ and $2x10^{-11}$ m^2. The gas at 760 ^{0}C (1033 K) enters the vessel tangentially into the shroud with a superficial velocity of 9.815 m/s and turbulence intensity of 5%. The air density, viscosity, and heat capacity are respectively 4.53 kg/m^3, 3.7 x 10^{-5} kg/m.s, 1006.4 J/kg K. The operating pressure was 1344 kPa.

5. Model:

The gas flow in the filter vessel is in a state of turbulence motion. It is, therefore, important to use an appropriate turbulence model for evaluating the mean flow field. The FLUENT^{TM} code provides options for using either the k-ε standard version or the Reynolds Stress Transport

Model (RSTM). While the k-ε model is widely used in industrial applications, it suffers from several shortcomings. Its use of an isotropic eddy viscosity limits its applicability and causes the model to be incapable of handling the turbulence normal stress effects. The RSTM, however, accounts for the evolution of individual turbulent stress components. Therefore, the RSTM entirely avoids the use of an eddy viscosity and is clearly well suited for handling anisotropic turbulence fluctuations. Following the work of Ahmadi and Smith (1998) and Zhang and Ahmadi (2001), the RSTM is used in this study.

For an incompressible fluid, the equations for the conservation of mass and momentum for the mean motion are given as

$$\frac{\partial \bar{u}_i}{\partial x_i} = 0 \tag{1}$$

$$\frac{\partial \bar{u}_i}{\partial t} + \bar{u}_j \frac{\partial \bar{u}_i}{\partial x_j} = -\frac{1}{\rho}\frac{\partial \bar{p}}{\partial x_i} + \vartheta \frac{\partial^2 \bar{u}_i}{\partial x_j^2} - \frac{\partial R_{ij}}{\partial x_j} \tag{2}$$

where $\bar{u}_i$ is the mean velocity, x_i is the position, t is the time, $\bar{p}$ is the mean pressure, ρ is the constant mass density, ϑ is the kinematic viscosity, and $R_{ij} = \overline{u'_i u'_j}$ is the Reynolds stress tensor. Here, $u'_i = u_i - \bar{u}_i$ is the fluid fluctuation velocity.

The Reynolds Stress Transport Model (RSTM) provides for differential transport equations for evaluation of the turbulence stress components, i.e.,

$$\frac{\partial R_{ij}}{\partial t} + \bar{u}_k \frac{\partial R_{ij}}{\partial x_k} = \frac{\partial}{\partial x_k}\left(\frac{\nu_t}{\sigma^k}\frac{\partial R_{ij}}{\partial x_k}\right) - \left[R_{ik}\frac{\partial \bar{u}_j}{\partial x_k} + R_{jk}\frac{\partial \bar{u}_i}{\partial x_k}\right] - C_1\frac{\varepsilon}{k}\left[R_{ij} - \frac{2}{3}\delta_{ij}k\right] - C_2\left[P_{ij} - \frac{2}{3}\delta_{ij}P\right] - \frac{2}{3}\delta_{ij}\varepsilon \tag{3}$$

where the turbulence production terms are defined as

$$P_{ij} = -R_{ik}\frac{\partial \bar{u}_j}{\partial x_k} - R_{jk}\frac{\partial \bar{u}_i}{\partial x_k}, \quad P = \frac{1}{2}P_{ij} \tag{4}$$

with P being the fluctuation kinetic energy production. Here $\sigma^k = 1.0$, $C_1 = 1.8$, $C_2 = 0.6$ are empirical constants (Launder *et al*. (1975)).

The transport equation for the turbulence dissipation rate, ε, is given as

$$\frac{\partial \varepsilon}{\partial t} + \bar{u}_j \frac{\partial \varepsilon}{\partial x_j} = \frac{\partial}{\partial x_j}\left[\left(\vartheta + \frac{\nu_t}{\sigma^\varepsilon}\right)\frac{\partial \varepsilon}{\partial x_j}\right] - C^{\varepsilon 1}\frac{\varepsilon}{k}R_{ij}\frac{\partial \bar{u}_i}{\partial x_j} - C^{\varepsilon 2}\frac{\varepsilon^2}{k} \tag{5}$$

In Equation (5), $k = \frac{1}{2}\overline{u'_i u'_i}$ is the turbulence kinetic energy, and ν_t is the "eddy" or turbulent viscosity. The values of constants are

$$\sigma^{\varepsilon} = 1.3, \quad C^{\varepsilon 1} = 1.44, \quad C^{\varepsilon 2} = 1.92 \tag{6}$$

The RSTM of the FLUENT^{TM} code and the standard wall function boundary condition were used for evaluating the mean velocity field and the Reynolds stresses in the filter vessel.

For the energy transport equation, we solved the convection-diffusion heat transfer equation given as

$$\frac{\partial \overline{T}}{\partial t} + \overline{u}_j \frac{\partial \overline{T}}{\partial x_j} = \frac{\partial}{\partial x_j}\left[\left(\alpha + \frac{\nu_t}{\sigma^T}\right)\frac{\partial \overline{T}}{\partial x_j}\right] \tag{7}$$

Here $\overline{T}$ is the mean temperature, α is the thermal conductivity and σ^T is the temperature turbulent Prandtl number.

In the solution procedure, we assume that the flow and heat transfer equations are decoupled. i.e., the properties are temperature-independent and the buoyancy force is negligible. Based on the decoupling assumption, we first solved the isothermal flow and obtained a converged flow field solution, and then solved the energy transport equation to find the temperature variation in the vessel.

6. Results and Discussion:

Figure 4 shows the grid generated by GAMBIT which is used in this study. Figure 4a shows the surface grid and Figure 4b shows the grid for the inner structure of the vessel. This figure displays the inlet, outlet, shroud, tube sheets, the effective upper and lower cylindrical filters, and the connecting post.

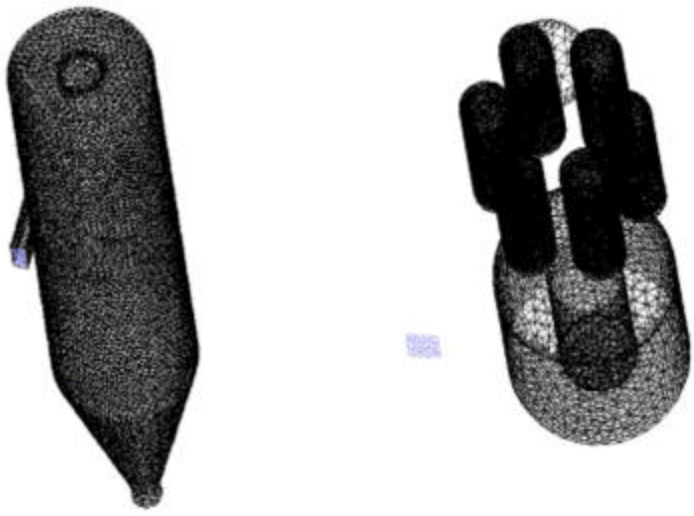

(a) **(b)**

Figure 4. The Computational Grid for the Filter Vessel –
(a) Outer Shell (b) Internal Strucutres

As stated before, the Reynolds Stress Transport turbulence model in addition to the heat transfer equation were used in these computations. In the simulation, the origin of the coordinate system is set in the center of the circle on top of the vessel. The z-axis is in the vertical direction (gravitational direction) and the x-axis is along the inlet flow direction. Figure 5 shows the gas temperature variation in the vessel. It is observed that the temperature is higher at the inlet (1033 K), cooler near the conical section and higher at the outlet. This trend is qualitatively consistent with the experimental findings of Guan (2000) for the filter vessel at Wilsonville.

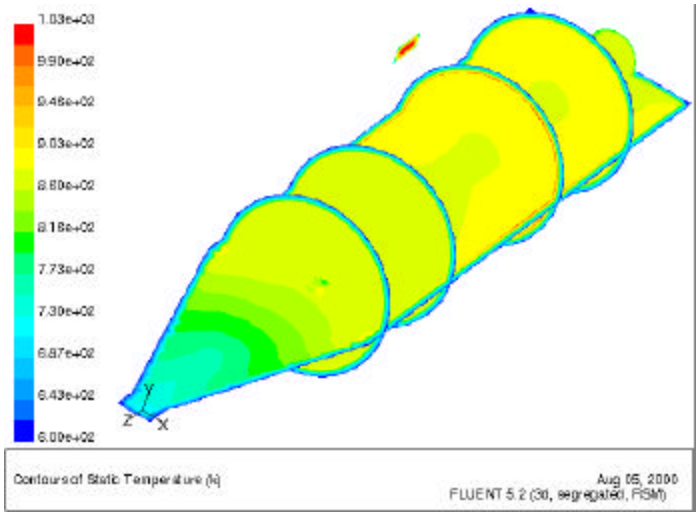

Figure 5. Gas Temperature Contours in the Filter Vessel

The contour plots for gas temperature gradients in various planes are shown in Figure 6. This figure confirms that the temperature is higher in the upper part of the filter vessel than in the lower part.

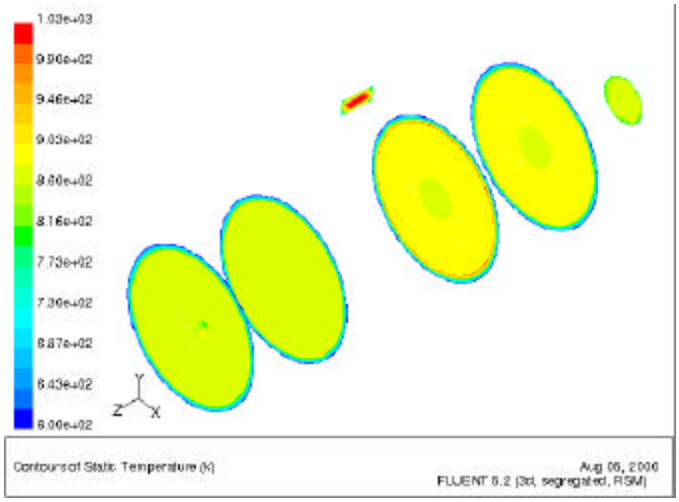

Figure 6. Gas Temperature Contours at Different Sections in the Filter Vessel

The contour plots for variations of the static pressure are shown in Figure 7. This figure shows that the pressure is roughly uniform inside the filter vessel (of about 25 kPa).

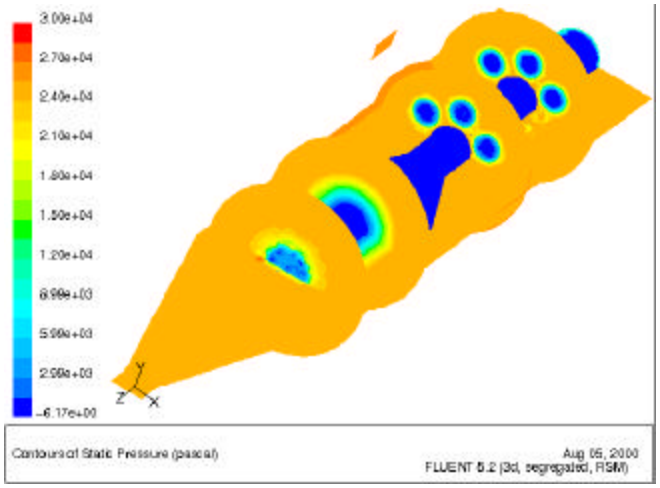

Figure 7. Gas Pressure Contours in the Filter Vessel

Figure 8 shows the static pressure at different cross sectional areas. This figure shows that the main pressure drop occurs across the candle filter walls and that the pressure reduces to about 29 kPa inside the filter cavity. The air pressure inside the filter cavity and connecting pipes is roughly constant with a slight decrease toward the vessel outlet. This observation is consistent with the earlier results of Zhang and Ahmadi (2001).

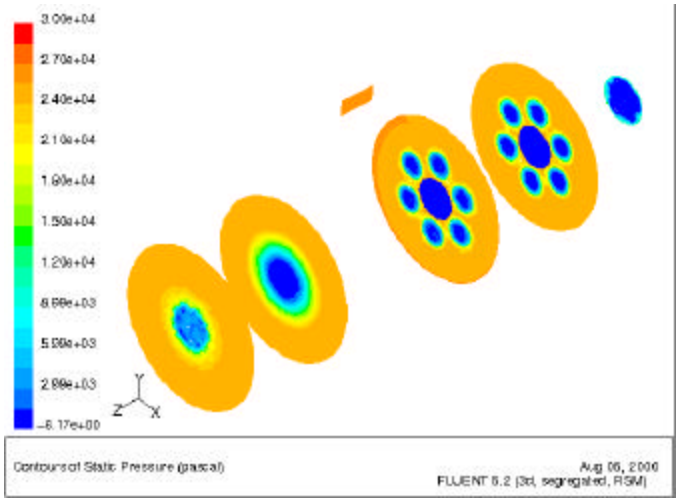

Figure 8. Gas Pressure Contours at Different Sections in the Filter Vessel.

The velocity vector fields in a plane across the filter vessel is shown in Figure 9. This figure shows that a strong rotating flow region occurs outside the shroud and inside the filter vessel

near the upper and lower parts. It is also observed from Figure 9 that the velocity is quite low inside the vessel.

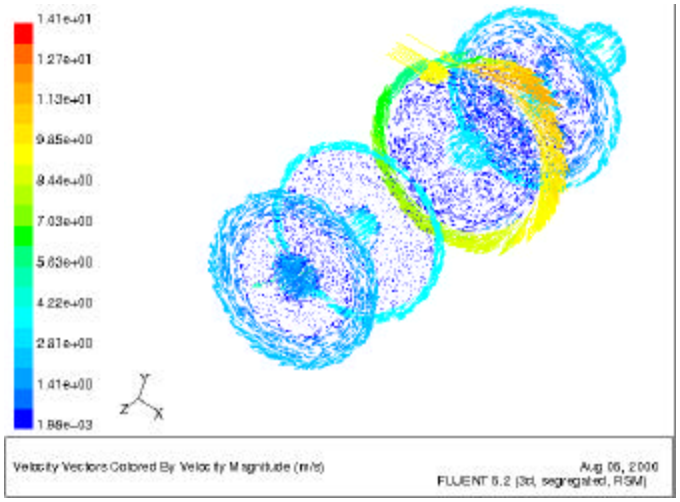

Figure 9. Velocity vector field in a plane across the filter vessel.

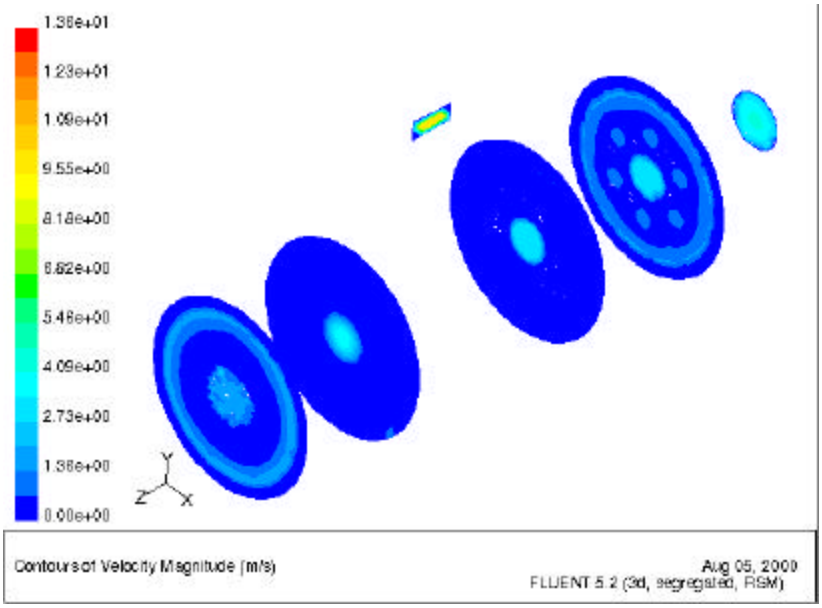

Figure 10. Velocity magnitude contour in the filter vessel.

The velocity magnitude contour shown in Figure 10 shows that the velocity is quite high at the inlet but becomes quite low in the body of the vessel. The velocity magnitude increases in the outlet pipe as the gas leaves the vessel.

7. Conclusions:

This study was undertaken to assess the gas temperature distribution in the Wilsonville filter vessel. The energy transport equation was used with the Reynolds Stress Transport Turbulence Model to simulate the gas flows in the Wilsonville Filter Vessel. The simulated gas temperature distributions in the vessel qualitatively agree with the experimental findings, showing non-isothermal conditions with higher temperature in the upper part of the filter and lower temperature near the cone. Strong rotating flow regions were also predicted inside the filter vessel near the upper and lower parts, which are also in agreement with the field observations. The pressure was found to be roughly uniform inside the filter vessel and the main pressure drop occurring across the candle filter vessel walls.

Acknowledgement

The authors would like to thank Xiaofeng Guan, and Howard Hendrix, of Southern Company Services, John Foote of Siemens Westinghouse, Theodore McMahon, Richard Dennis, and Tom O'Brien for many helpful discussions on the filter vessel. Thanks are also given to Hiafeng Zhang and Richard Anderson for their assistance. G. Ahmadi work was supported by the DOE grant DE-FC26-98T4047. Thanks to FLUENT^{TM} Corporation for making the code available. Special thanks to Xiaofeng Guan for his in-depth review and constructive comments on this manuscript.

References

Ahmadi, G., and Zhang, H., Hot-Gas Flow and Particle Transport and Deposition in the Filter Vessel at Wilsonville, *Proceedings of Seventeenth Annual International Pittsburgh Coal Conference*, Pittsburgh, PA, September 11-14, 2000.

Ahmadi, G., and Smith, D.H., Particle Transport and Deposition in a Hot-Gas Cleanup Pilot Plant, *Aerosol Science and Technology*, **29**:183-205, 1998a.

Ahmadi, G., and Smith, D. H., Gas Flow and Particle Deposition in the Hot-Gas Filter Vessel at the Tidd 70 MWE PFBC Demonstration Power Plant *Aerosol Science and Technology*, **29**, 206-223, 1998b.

Dahlin, R. S., Lendham, E. C., and Hendrix, H. L., In Situ Particulate Sampling and Ash

Characterization at the Power Systems Development Facility, *Aerosol Science and Technology*, **29**:170-182, 1998.

Ferer, M., and Smith, D. H., Modeling of Filter Cleaning: The Small-Particle Filter-Cake Fragments, *Aerosol Science and Technology*, **29**:246-256, 1998.

Guan, X., Personal Communication, July 26, 2000.

He, C. and Ahmadi, G., Particle Deposition in a nearly Developed Turbulent Duct Flow with Electrophoresis, *Journal of Aerosol Science*, **30**, 793-758, 1999.

Kono, H. O., Richman, L. M., Jordan, B. R., and Smith, D. H., Filter-Cake Property Characterization for Hot Gas Candle Filters, *Aerosol Science and Technology*, **29**:236-245, 1998.

Li, A., Ahmadi, G., Bayer, R. G., and Gaynes, M. A., Aerosol Particle Deposition in an Obstructed Turbulent Duct Flow, *J. Aerosol Science*, **25**:91-112, 1994.

Lippert, T. E., Bruck, G. J. Sanjana, Z. N., and Newby, R. A., Westinghouse Advanced Particle Filter System, *Proceedings of Advanced Coal-Fired Power System '95*, Review Meeting, DOE/METC-95/10108, Morgantown Energy Technology Center, Morgantown, WV, June 27-29, 123-139, 1995.

Radian Corporation, *A Study of Hazardous Air Pollutants at the Tidd PFBC Demonstration Plant*, DCN 94-633-021-03. Morgantown Energy Technology Center, Morgantown, WV, 1994.

Smith, D. H., Haddad, G. J., and Grimm, U., Composition and Chemistry of Particulates from a PFBC Demonstration Plant, *Fuel*, **76**:727-732, 1997a.

Smith, D. H., Haddad, G. J., and Ferer, M., Shear Strengths of Heated and Unheated Mixtures of $MgSO_4$ and $CaSO_4$ Powders. Model Pressurized Fluidized Bed Combustion Filter Cakes, *Energy & Fuels*, **11**:1006-1011, 1997b.

Smith, D. H., Powell, V., Ahmadi, G., and Ferer, M., Analysis of Operational Filtration Data-Part III. Re-entrainment and Incomplete Cleaning of Dust Cake, *Aerosol Science and Technology*, **29**:224 235, 1998.

Smith, D. H. and Ahmadi, G., Problems and Progress in Hot-Gas Filtration for Pressurized Fluidized Bed Combustion (PFBC) and Integrated Gasification Combined Cycle (IGCC), *Aerosol Science and Technology*, **29**:224-235, 1998.

Zhang, H., and Ahmadi, G., Particle Transport and Deposition in the Hot-Gas Filter Vessel at Wilsonville, *Powder Technology*, **In Press,** 2001.